

2025 IEEE International Multi-Conference on Smart Systems & Green Process

CERTIFICATE OF PARTICIPATION

This is to certify that:

Messaoud Garah

Has participated in the 2025 IEEE International Multi-Conference on Smart Systems & Green Process held on October 30 - November 02, 2025, Hammamet-Tunisia, with the paper entitled:

“A Novel Design of a Wilkinson Power Divider for Dual-Band Operation”

Authors: Messaoud Garah, Elhadi Kenane, Amal Sila

[Handwritten signature]

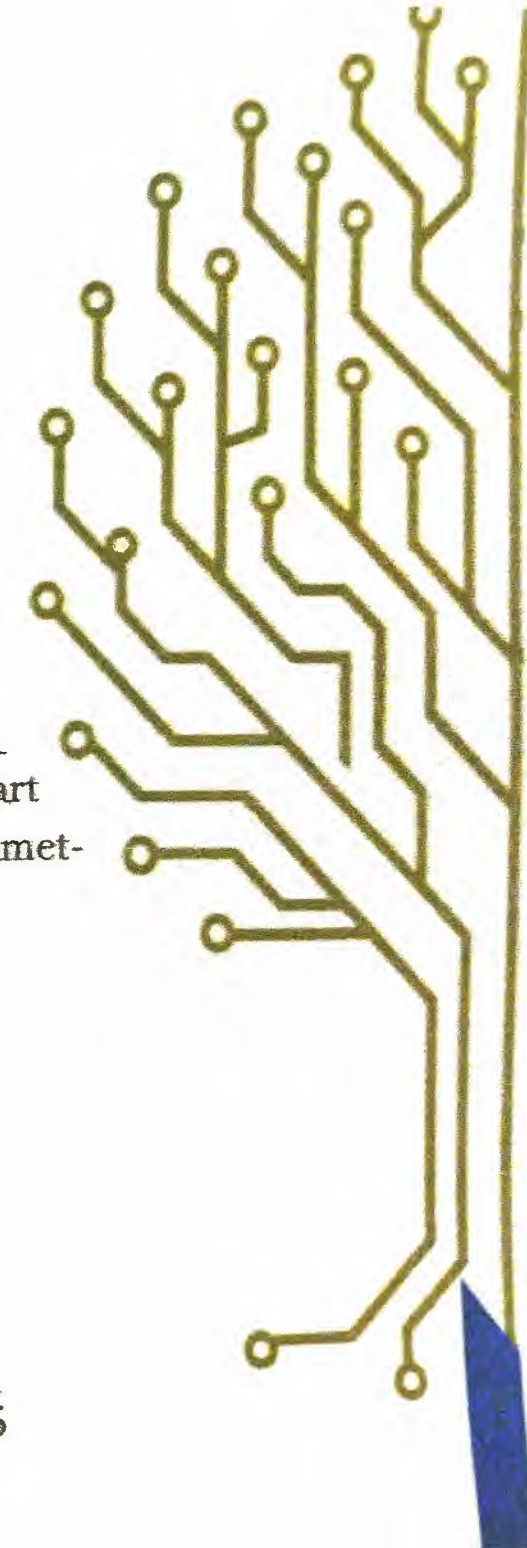
General Chair

Prof. Mohamed Naceur ABDELKRIM



Date

02 November 2025



A Novel Design of a Wilkinson Power Divider for Dual-Band Operation

Messaoud Garah

Electronic Department, LGE
Laboratory

University Mohamed Boudiccf M'sila
University Pole, Road Bourdj Bou
Arriridj, M'sila 28000, Algeria
messaoud.garah@univ-msila.dz

Elhadi Kenane

Electronic Department, LGE
Laboratory

University Mohamed Boudiccf M'sila
University Pole, Road Bourdj Bou
Arriridj, M'sila 28000, Algeria
elhadi.kinane@univ-msila.dz

Amal Sila

Electronic Department, LGE
Laboratory

University Mohamed Boudiccf M'sila
University Pole, Road Bourdj Bou
Arriridj, M'sila 28000, Algeria
amal.sila@univ-msila.dz

Abstract—This paper presents a novel design of a Wilkinson power divider for dual-band operation. In the proposed design, the conventional two quarter-wavelength transmission lines are replaced with two stubs connected by a single coupled line. Additionally, an isolation resistor is connected between the two output ports. Using even–odd mode analysis and the ABCD matrix method, the design equations for the proposed circuit are derived. The divider is fabricated on an FR-4 substrate with a dielectric constant of 4.3 and a thickness of 0.8 mm. Simulation results show that the divider achieves good performance at both design frequencies, 0.85 GHz and 2.3 GHz, with low return loss at all ports (S_{11} , S_{22} , and S_{33}), good transmission coefficients (S_{21} and S_{31}), and high isolation (S_{23}) between the two output ports.

Keywords— Dual-Band, Even-Odd mode Analysis, Isolation Loss, Wilkinson Power Divider.

I. INTRODUCTION

Many microwave and millimeter-wave circuits, including antenna feeding networks [1], RF mixers [2], and power amplifiers [3], require power dividers (PDs) or combiners. One of the most predominant types of PDs is the Wilkinson power divider (WPD), invented in 1960 by Ernest Wilkinson [4]. This divider is designed to split the input power from a single port into two or more output ports. It can be used for both equal and unequal power division.

The conventional WPD is a three-port network composed of two quarter-wavelength ($\lambda/4$) transmission line sections and an isolation resistor of $2Z_0$ connected between the two output ports, as illustrated in Fig.1. The Wilkinson divider is particularly notable due to its importance characteristics, which include a simple design, impedance matching at all ports, and high isolation between output ports. However, its main disadvantages are its large physical size and narrow bandwidth, especially at lower operating frequencies.

Modern wireless communication systems demand dual-band operation and miniaturized power dividers. To meet these requirements, numerous concepts and technologies for designing dual-band, multi-band, and compact WPDs have been developed in recent years. For instance, [5] presents a compact dual-band WPD that uses a common inductor and a complex load with lumped transmission lines. This approach achieves port matching at both frequency bands and significantly reduces the WPD's overall physical size compared to a conventional design. Additionally, paper [6] demonstrates a compact dual-band WPD realized using a cascaded π -shape structure and dual transmission lines. The divider proposed in [7] replaces the conventional $\lambda/4$ transmission line with simplified L-type transmission lines.

This modification enhances the frequency ratio, bandwidth, and isolation. In [8], a dual-band WPD is implemented using dual coupled lines and a pair of open stubs, achieving good performance across the two frequency bands. Similarly, [11] employs multi-section coupled-line structures to provide both dual-band and wide-band operations. Lastly, [12] introduces a tri-band WPD that incorporates a quarter-wave open stub along its $50\ \Omega$ output ports to enable multi-band operations.

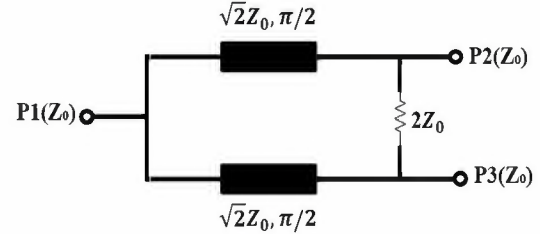


Fig. 1. Conventional WPD.

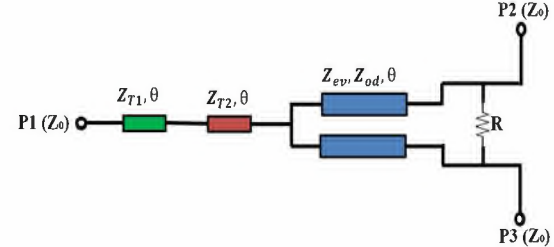


Fig. 2. Structure of the proposed WPD for dual-band operation.

In our previous work, we introduced a four-port dual-band WPD [13]. This paper presents an optimized and parametric study of that design. The results show that the divider exhibits good performance at both WLAN frequency bands (2.45 GHz and 5.8 GHz). Additionally, [14] proposed the design and simulation of coupled-line WPD. In this configuration, the two conventional $\lambda/4$ transmission lines are replaced with a single coupled line, which offers several advantages, such as compact size design, impedance matching at all ports, and high isolation.

This work presents a novel design and simulation of a compact WPD for dual-band operation. The proposed structure is composed of two stubs; a single coupled line, and an isolation resistor connected between the two output ports. The design equations of the proposed WPD are derived through theoretical analysis using even–odd mode analysis and the ABCD matrix method. The proposed design is simulated using CST Studio Suite simulator and fabricated on

an FR-4 substrate with dielectric constant ϵ_r of 4.3 and a thickness h of 0.8 mm.

This paper is organized as follows: Section 1 provides the introduction; the design analysis of the proposed design is described in Section 2; Section 3 presents the simulation setup and discusses the obtained results. Section 4 concludes the paper.

II. PROPOSED CIRCUIT AND DESIGN EQUATIONS

Fig. 2 illustrates the structure of the proposed WPD. The circuit comprises two stubs with characteristic impedances (Z_{T1} and Z_{T2}), and a single coupled line with even- and odd-mode characteristic impedances (Z_{ev} and Z_{od}), which replaces the two quarter-wavelength transmission lines used in the conventional divider. The isolation network consists of a lumped resistor R connecting the two output ports.

To achieve dual-band operation, the electrical length of all transmission lines at both operating frequencies (f_1 and f_2) should satisfy (1) and (2)

$$\theta_{f1} = \frac{\pi}{(1+U)} \text{ and } \theta_{f2} = \frac{U\pi}{(1+U)} \quad (1)$$

where

$$U = \frac{\theta_2}{\theta_1} = \frac{f_2}{f_1} \quad (2)$$

The parameter U represents the frequency ratio, and θ_1 and θ_2 are the electrical lengths corresponding to the two operating frequencies.

A. Even-Mode

To achieve input port matching of the Wilkinson divider, the even-mode circuit must be matched; the circuit in Fig. 2 can be simplified to the equivalent half circuit shown in Fig. 3.

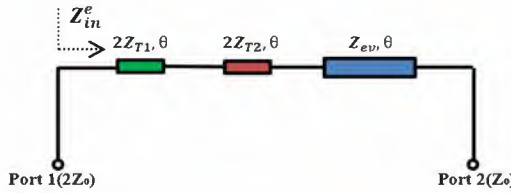


Fig. 3. Equivalent half circuit of the proposed WPD for dual-band operation under even-mode excitation.

The ABCD matrix of the even-mode equivalent circuit is expressed as follows:

$$\begin{bmatrix} A & B \\ C & D \end{bmatrix} = \begin{bmatrix} \cos \theta & j2Z_{T1} \sin \theta \\ j \frac{\sin \theta}{2Z_{T1}} & \cos \theta \end{bmatrix} \times \begin{bmatrix} \cos \theta & j2Z_{T2} \sin \theta \\ j \frac{\sin \theta}{2Z_{T2}} & \cos \theta \end{bmatrix} \times \begin{bmatrix} \cos \theta & jZ_{ev} \sin \theta \\ j \frac{\sin \theta}{Z_{ev}} & \cos \theta \end{bmatrix} = \begin{bmatrix} 0 & j\sqrt{2}Z_0 \\ j \frac{1}{\sqrt{2}Z_0} & 0 \end{bmatrix} \quad (3)$$

After some mathematical manipulation, each element of the ABCD matrix in (3) is obtained as:

$$A = 1 - \frac{Z_{T1}}{Z_{T2}} \tan^2 \theta - \frac{2}{Z_{ev}} \tan^2 \theta (Z_{T2} + Z_{T1}) \quad (4a)$$

$$B = j(Z_{ev} + 2Z_{T2} + 2Z_{T1}) \sin \theta \cos^2 \theta - j \frac{Z_{T1}Z_{ev}}{Z_{T2}} \sin^3 \theta \quad (4b)$$

$$C = j \left(\frac{1}{Z_{ev}} + \frac{1}{2Z_{T2}} + \frac{1}{2Z_{T1}} \right) \sin \theta \cos^2 \theta - j \frac{Z_{T2}}{Z_{T1}Z_{ev}} \sin^3 \theta \quad (4c)$$

$$D = 1 - \frac{Z_{T2}}{Z_{T1}} \tan^2 \theta - Z_{ev} \tan^2 \theta \left(\frac{1}{2Z_{T2}} + \frac{1}{2Z_{T1}} \right) \quad (4d)$$

By solving equation (4), the value of the characteristic impedance Z_{ev} is given by:

$$Z_{ev} = 2Z_{T2} \frac{Z_{T1} \cot^2 \theta + Z_{T2} \tan^2 \theta - Z_{T2}Z_{T1} \tan^2 \theta}{Z_{T2} \cot^2 \theta + Z_{T1} \tan^2 \theta - Z_{T2}Z_{T1} \tan^2 \theta} \quad (5)$$

B. Odd-mode

The odd-mode equivalent circuit of the proposed WPD is shown in Fig. 4.

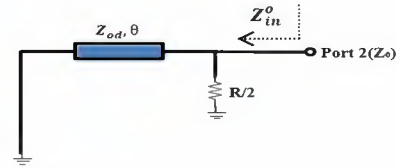


Fig. 4. Equivalent half circuit of the proposed WPD for dual-band operation under odd-mode excitation.

The ABCD matrix of the odd-mode equivalent circuit is derived as:

$$\begin{bmatrix} A & B \\ C & D \end{bmatrix} = \begin{bmatrix} \cos \theta & jZ_{od} \sin \theta \\ j \frac{\sin \theta}{Z_{od}} & \cos \theta \end{bmatrix} \begin{bmatrix} 1 & 0 \\ \frac{2}{R} & 1 \end{bmatrix} \quad (6)$$

The above matrix equation can be simplified as follows:

$$\begin{bmatrix} A & B \\ C & D \end{bmatrix} = \begin{bmatrix} \cos \theta + j2 \frac{Z_{od}}{R} \sin \theta & jZ_{od} \sin \theta \\ j \frac{1}{Z_{od}} \sin \theta + \frac{2}{R} \cos \theta & \cos \theta \end{bmatrix} \quad (7)$$

The characteristic impedance of the odd-mode can be calculated as:

$$Z_{in}^o = \frac{j2Z_{od} \tan \theta}{R + j2Z_{od} \sin \theta} = Z_0 \quad (8)$$

From (7) and (8), we obtain:

$$R = 2Z_0 \quad (9)$$

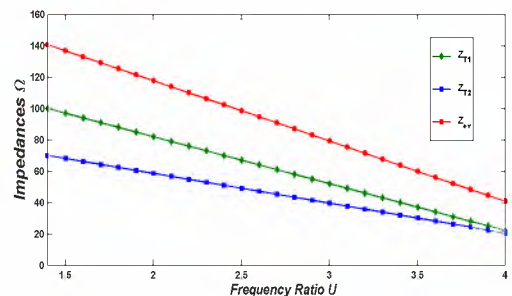


Fig. 5. Design parameters of the proposed WPD for dual-band operation versus frequency ratio U .

Fig. 5 shows the variation of the calculated design parameters as a function of the frequency ratio U . As observed, an increase in the frequency ratio leads to a decrease in the values of all impedances (Z_{T1} , Z_{T2} and Z_{ev}). The proposed WPD can operate effectively within a frequency ratio range of 1.4 to 5. This performance is achievable if the characteristic impedances of the first and the second stubs (Z_{T1} and Z_{T2}) are limited to the ranges of $20-100 \Omega$ and $20-70 \Omega$, respectively. Additionally, the characteristic impedance of the coupled line is limited to a range of $40-140 \Omega$. Furthermore, when the frequency ratio is $U=2.7$, the proposed WPD operates at two distinct frequency bands: $f_1 = 0.85 \text{ GHz}$ and $f_2 = 2.3 \text{ GHz}$. In this case, the characteristic impedances of each transmission line are calculated as: $Z_{T1} = 58.33 \Omega$, $Z_{T2} = 45.03 \Omega$, $Z_{ev} = 83.51 \Omega$, $Z_{od} = 66.11 \Omega$, and $R = 100 \Omega$.

III. SIMULATION DESIGN AND RESULTS ANALYSIS

The proposed WPD is designed and simulated for dual-band operation at 0.85 GHz and 2.3 GHz , which is dedicated to 5G applications. The novel divider is fabricated on FR-4 substrate with a complete ground plane on the bottom layer, as shown in Fig. 6. The substrate has a relative dielectric constant of $\epsilon_r = 4.3$ and a thickness of 0.8 mm , while the ground plane is a $35 \mu\text{m}$ thick copper layer. The dimensions of both the substrate and the ground plan are $60 \times 38 \text{ mm}^2$. The physical dimensions of the designed layer are listed in Table 1.

TABLE I. PHYSICAL DIMENSIONS OF THE PROPOSED WPD FOR DUAL-BAND OPERATION

Parameters	Values (mm)
W_{p1}	1.5
W_{p2}	1.5
L_p	9.5
W_{T1}	1.15
L_{T1}	23
W_{T2}	1.8
L_{T2}	22
W_{cp}	0.67
L_{cp}	30
S	1.1

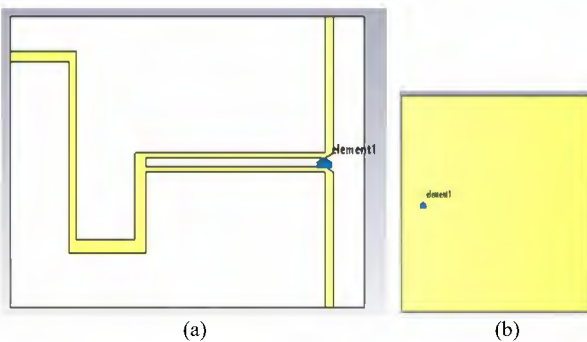


Fig. 6. Proposed model of the WPD for dual-band operation using CST simulator: (a) Top view and (b) Bottom view.

In this section, the simulation results of the proposed WPD for dual-band operation are obtained using CST simulator V2021. The simulated S-parameters of the novel design are plotted in Fig. 7. From Fig. 7 (a), the input return loss (S_{11}) is below -20 dB for the first operating band at 0.85 GHz and below -30 dB for the second band at 2.3 GHz . Additionally, the output return losses (S_{22} and S_{33}) are all below -15 dB at both design frequencies. The transmission coefficients (S_{21} and S_{31}) are approximately -3 dB for both frequency bands with a deviation of 0.2 dB at the first frequency band and 0.3 dB at the second, as shown in Fig. 7 (b). Furthermore, it is observed that the isolation (S_{23}) is less than -15 dB at both operating frequencies.

To demonstrate the advantages of our proposed design, Table 2 summarizes a comparison between our divider and previous published dual-band WPDs. It was found that the proposed design has a simpler topology than other works and enhance the performance factors such as return loss, transmission parameters and isolation loss. Furthermore, the proposed divider operates at frequencies of 0.85 and 2.3 GHz , which are significant in modern wireless communications.

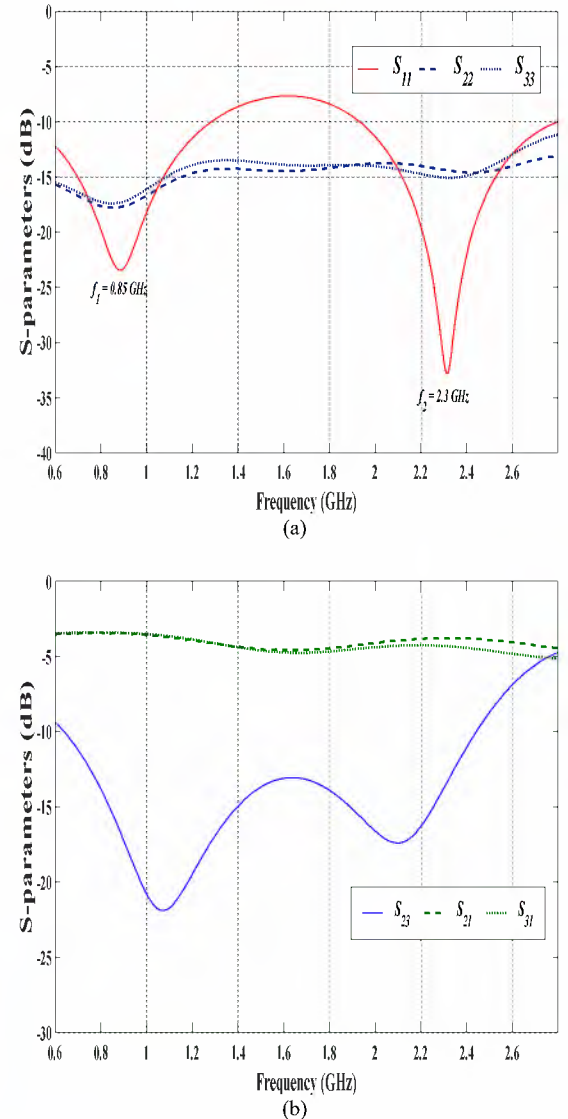


Fig. 7. Simulated parameters of the proposed WPD for dual-band operation. (a) Input and output return loss, (b) Transmission parameters and isolation loss.

TABLE II. COMPARISONS BETWEEN PREVIOUS PUBLISHED DUAL-BAND WPDs WITH THIS WORK

Referenes	Operating Frequency f_1/f_2	Topology	Retun Loss $ S_{11} (\text{dB})$	Transmission Parameters $ S_{21} , S_{31} (\text{dB})$	Isolation Loss $ S_{23} (\text{dB})$
[7]	1/3.5 GHz	5-TLs & 1-R 5-TLs & 2-stubs 1-R	27/25	3.4/3.4	25/20
[8]	0.5/2.25 GHz	2-CL, 2-OS and 1-R	28/25	3.3/3.3	25/25
[9]	0.9/2.45 GHz	4-TLs, 2- short CRLH TLs and 1-R	23.7/17.0	3.19/3.18	20/15
[10]	1/2 GHz	4-TLs and 1-RLC	20/25	3.14/3.19	20/15
This work	0.85/2.3 GHz	2-TLs, 1-CL and 1-R	22/31	3.2/3.3	20/15

TLs: Transmission Lines, R: Resistor, CL: Coupled Line, OS: Open Stub, CRLH: Composite Right-Left Handed and RLC: Resistor-Inductor-Capacitor.

IV. CONCLUSION

In this paper, a novel Wilkinson power divider (WPD) is proposed for dual-band operation with a compact size. Theoretical analysis using the even-odd mode and the ABCD matrix has been carried out to determine the design equations and parameters. The use of coupled line and stubs in the proposed design provides several benefits, including a simpler structure, a wider operating range, and a more compact size. Simulation results show good performance in terms of compactness, impedance matching at all ports, favorable transmission characteristics, and high isolation at both frequency bands. Finally, the theoretical and simulated results are in very good agreement.

ACKNOWLEDGMENT

This work was supported by the Algerian Ministry of Higher Education and Scientific Research via funding through the PRFU project no. A25N01UN280120230002.

REFERENCES

- [1] M. -A. Chung, D. Udris, C. -W. Lin, and C. -W. Yang “A 28-GHz Vivaldi Antenna with Power Divider Structure for Achieving Wide Band and Gain Enhancement,” International Journal of Antennas and Propogation, vol. 2024, no. 1, January 2024.
- [2] K. Yoon, and K. G. Kim, “Miniatrization of a single-ended mixer using T-shaped Wilkinson power combiner for medical wireless communication applications,” Microwave Opt. Technol. Lett., vol. 61, no. 8, pp. 1977-1982, February 2019.
- [3] I. G. G. Ary, G. N. Kamucha, and F. Manene, “Design of a High-Efficiency Doherty Power Amplifier for 5G Applications Using Wilkinson power Dividers,” Journal of Communications, vol. 17, no. 8, pp. 675-681, 2022.
- [4] E. J. Wilikinson, “An N-Way Hybrid Power Divider,” IEEE Trans. Microwave Theory Tech, vol. 8, no. 1, pp. 116-118, January 1960.
- [5] C. Pakasiri, and S. Wang, “Dual-Band Compact Wilkinson Power Divider Using Common Inductor and Complex Load,” IEEE Access, vol. 8, pp. 97189-97195, 2020.
- [6] M. Kumar, S. K. Parui, and S. Das, “Design of Miniaturized Dual-Band Wilkinson Power Divider Using Dual and Cascade Pi-Shaped Transmission Lines,” Radioengineering, vol. 27, no. 4, pp. 1056-1063, September 2018.
- [7] F. -X. Liu, and J. -C. Lee, “Design of New Dual-Band Wilkinson Power Dividers with Simple Structure and Wide Isolation,” IEEE Trans. Microwave Theory Tech, vol. 67, no. 9, pp. 3628-3635, September 2019.
- [8] W. Zhao, N. Zhang, B. Wu, X. Wang, Z. Ma, and C. -P. Chen, “A Dual-Band Wilkinson Power Divider Using Dual Coupled Lines and Open Stubs,” 2020 IEEE MTT-S International Wireless Symposium (IWS), pp. 1-3, September 2020.
- [9] M. Zhao, A. Kumar, C. Wang, B. Xie, T. Qiang, and K. K. Adhikari, “Design method of dual-band Wilkinson power divider with improved out-of-band rejection performance and high design flexibility,” AEU - International Journal of Electronics and Communications, vol. 110, pp. 152844, October 2019.
- [10] T. -J. Chang, Y. -F. Tsao, T. -J. Huang, and H. -T. Hsu, “Bandwidth Improvement of Conventional Dual-Band Power Divider Using Physical Port Separation,” Electronics, vol. 9, no. 12, pp. 2192, December 2020.
- [11] A. I. Omi, R. Islam, M. A. Maktoomi, C. Zakzewski and P. Sekhar, “A Novel Analytical Design Technique for Wideband Wilkinson power Divider Using Dual-Band Technology,” Sensors, vol. 21, no. 19, pp. 6330, September 2021.
- [12] B. M. abdelrahman, H. N. Ahmed, and A. I. Nashed, “A Novel Tri-Band Wilkinson Power Divider for Multiband Wireless Applications,” IEEE Microwave Wireless Compon. Lett, vol. 27, no. 10, pp. 891-893, October 2017.
- [13] E. Kenane, M. Garah, and F. Benmeddour, “Parametric Study and Optimzation of a Dual-Band Four Ports Wilkinson Power Divider,” International Journal of Information Science and Technology, vol. 6, no. 1, pp. 4-13, February 2022.
- [14] A. Sila, M. Garah, E. Kenane, R. Guernine and R. Seghouri, “Design of Coupled-Line Wilkinson power Divider for UMTS mobile applications,” 2024 International Conference on Advanced in Electrical and Communication Technologies (ICAFCOT), pp. 1-4, October 2024.